ELSEVIER

Physica E 13 (2002) 451–454

PHYSICA E

www.elsevier.com/locate/physe

Organic microcavities based on thermally evaporated TeO_x-LiF dielectric mirrors

M. Anni[a,*], G. Gigli[a], S. Patanè[b], A. Arena[b], M. Allegrini[c], R. Cingolani[a]

[a] *National Nanotechnology Laboratory, Dipartimento di Ingegneria dell'Innovazione, Instituto Nazionale di Fisica della Materia (INFM), Università di Lecce, Via per Arnesano, 73100 Lecce, Italy*

[b] *Dipartimento Fisica della Materia e Tecnologie Fisiche Avanzate, Instituto Nazionale Fisica per Materia (INFM), Università di Messina, Salita Sperone 31, 98166 Sant'Agata-Messina, Italy*

[c] *Dipartimento di Fisica, Instituto Nazionale di Fisica per la Materia, Università di Pisa, Via F. Buonarroti n. 2 Pisa, Italy*

Abstract

We report on the realization of high-quality organic microcavities consisting of distributed Bragg reflectors (DBRs) based on lithium fluoride (LiF) and tellurium dioxide (TeO_x) deposited by thermal evaporation. The materials are transparent in the range from 350 nm to 5 μm and have an evaporation temperature of about 1000 K. The large difference in the refractive index (about 0.9 in the visible and near infrared range) allows one to obtain a reflectivity higher than 99% over a spectral region about 200 nm wide with a small number of periods. The mirror deposition technique is suitable for the fabrication of organic quantum microcavities in a single deposition process. Three fully evaporated organic λ cavities with Phyrrometene 580 as active material are described. The cavities show Q-value up to 300, good uniformity and reproducibility. © 2002 Elsevier Science B.V. All rights reserved.

Keywords: Vacuum deposition; Organics; Microcavity

Organic semiconductors have recently attracted much attention for application in electroluminescent devices such as light emitting diodes (LEDs) and displays. In this frame organic microcavity structures can be used to obtain a full control of the emission energy, linewidth, intensity and directionality for LED [1–9] as well as to obtain the optical feedback in laser resonators [10,11]. The commonly studied organic microcavities are realized by cladding the active material between a distributed Bragg reflector (DBR) and an evaporated metallic mirror [11–15], or by high-temperature mechanical pressing of two half DBR cavities [16]. To date, many different techniques and many different materials have been used for wide bandwidth DBR deposition to be used in organic cavities, such as SiO_2–Si_xN_y by plasma enhanced chemical vapor deposition (PECVD) [8,12–14], CF–CF(Au) by sputtering [17] and MgF_2–ZrO_2 by laser-induced vapor deposition [18]. These techniques cannot be used in the presence of the organic active material, thus requiring a complicated multi-step process for the realization of the cavity.

In this work, we report on the realization of organic dielectric microcavity entirely based on low-cost thermal evaporation of lithium fluoride (LiF) as the low refractive index material and tellurium oxide (TeO_x) as the high refractive index material. This approach allows us to realize highly reproducible and ultra low-cost mirrors. The high difference in

* Corresponding author. Tel.: +390-832-320-340; fax: +390-832-326-351.

E-mail address: marco.anni@unile.it (M. Anni).

PII: S1386-9477(02)00159-5

the refractive index of the two materials allows us to obtain reflectivity higher than 98% with a small number of periods, and to obtain a wide stopping band with a full-width at half-maximum (FWHM) of about 200 nm. Moreover, this permits to grow fully evaporated microcavities in a single step process.

As demonstrators, we have realized three different λ quantum microcavities with Pyrromethene 580 as active material, and increasing Q-value. We obtained a FWHM of the mode as low as 1.9 nm and a cavity Q-value of about 300. Angular dependent reflectivity is measured to probe the cavity mode for different longitudinal wavenumbers. The mode energy shows a blue shift as the incidence angle increases, consistent with the theoretical photon-like dispersion inside the cavity. The cavity uniformity, probed by mapping the reflectivity in different positions across the sample surface, is very good, despite the large sample dimension (about 25 mm^2) and the absence of a rotating sample holder in the evaporation chamber.

The DBRs are realized by thermal evaporation of $\lambda/4$ stacks of TeO_x/LiF on a Corning 5049 glass substrate and designed to show a maximum of reflectivity at 580 nm. The refractive index of the two materials has been determined by means of transmittance and the reflectance spectra, and turned out to be about 2.25 for TeO_x and about 1.39 for LiF in the wavelength range of interest. The materials are almost completely transparent in the range from 330 nm to 5 μm, thus they can be used for realization of dielectric mirrors in the entire visible and near infrared range. The evaporation temperature is 1140 K for LiF and 1006 K for TeO_x. The thickness of the layers is monitored in situ by a quartz oscillator microbalance maintaining the growth rate almost constant to 0.5 A s^{-1} to improve the film morphology. The high refractive index mismatch allows us to obtain reflectivity higher than 98% over a wide spectral region with a small number of periods. The reflectivity of an 8-period mirror is shown in Fig. 1 (dashed line), together with the theoretical spectrum (solid line) calculated by a transfer matrix model. The maximum reflectivity value is about 98.5%, and the stopping band is 160 nm wide.

As demonstrators we have realized three microcavities with output coupler of increasing reflectance, using Pyrromethene 580 as active material.

The bottom mirror is the same for all the cavities and consists on 8 TeO_x/LiF periods. The λ cavity is obtained by evaporating 200 nm of LiF on the bottom mirror, followed by a layer of Phyrromethene 580 of thickness of about 4 nm, and by a second 200 nm thick layer of LiF. The structure is completed by the evaporation of the top mirror, consisting of 6, 7 or 8 periods in the three different samples, respectively.

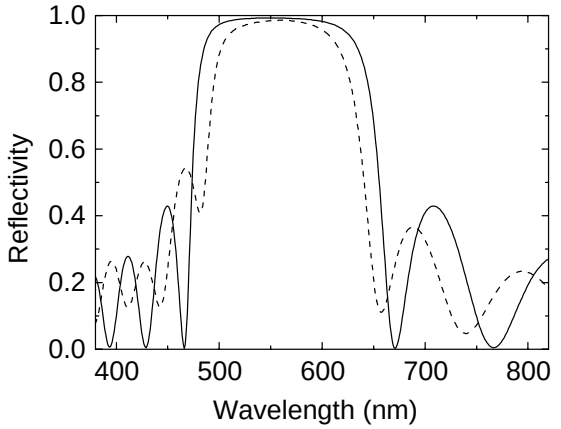

Fig. 1. Reflectivity of an 8-period LiF/TeO_x DBR calculated by the transfer matrix model (solid line) and experimental data from a real structure designed with the same parameters of the simulation. The peak reflectivity is 98.5% while the stopping band is 160 nm wide.

The spectral properties of the cavities have been probed through reflectance measurements. The reflectivity spectra of the three cavities in the stopping band spectral region are reported in Fig. 2. Two main features can be observed in the spectra:

(1) The mode linewidth continuously decreases, from 2.7 nm for the 6-period top mirror, to 1.9 nm for the 8-period top mirror; this effect is clearly ascribed to the rising of the Q-value of the cavity, due to the increasing output coupler reflectivity. The Q-value of the cavities is 215, 270 and 300 for the 6-, 7- and 8-period output coupler, respectively.

(2) The mode wavelength blue shifts, from 578 nm for a 6-period top mirror to 560 nm for an 8-period top mirror, as the top mirror reflectivity increases. This feature is not a direct effect of the increasing top mirror reflectance, but it is instead due to a systematic variation of the λ layer thickness along the sample holder surface arising from the non-uniform beam shapes, which generates the

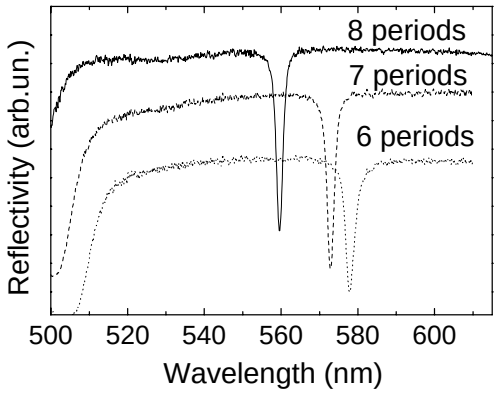

Fig. 2. Reflectivity in the DBR stopping band of the three cavities with 6-, 7- and 8-period top mirrors. The spectra are vertically translated for clarity. The mode FWHM is 2.7 nm in the cavity with a 6-period top mirror, 2.3 nm in the cavity with 7-period top mirror and 1.9 nm in the cavity with 8-period top mirror, corresponding to a cavity Q-value of 215, 270 and 300, respectively.

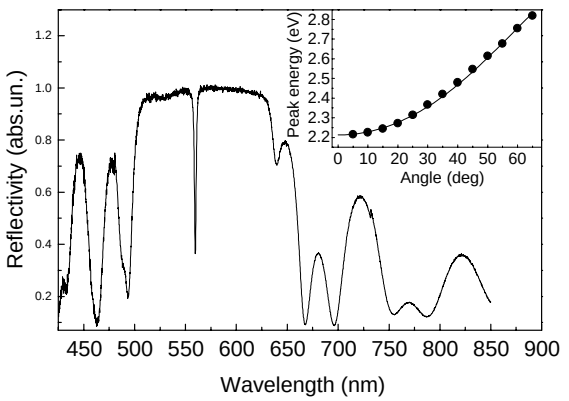

Fig. 3. Reflectivity spectrum of the 8-period top mirror cavity for normal incidence. The stopping band FWHM is about 160 nm. Inset: mode energy as a function of the angle of incidence. The continuous line is the best-fit curve with a photon-like dispersion curve obtained for a cavity energy at normal incidence $E_0 = 2.212 \pm 0.001$ eV and a cavity effective refractive index $n = 1.451 \pm 0.002$.

observed relative detuning of the three cavities, grown together in the same evaporation process.

Angle dependent reflectivity measurements were performed to probe the spectral properties of the highest Q-value cavity for different longitudinal wave vectors. The reflectivity spectrum of this cavity at normal incidence is shown in Fig. 3 and it displays

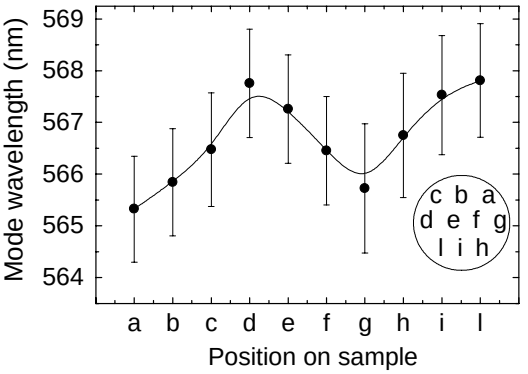

Fig. 4. Mode wavelength as a function of the position on the sample surface. The mode FWHM is taken as error bar. The overall maximum variation of about 2.4 nm reflects the good uniformity of the sample despite the dimensions of about 25 mm^2. Inset: actual position of points a, b, …, l on the sample surface.

a maximum value of 99.94% with a stopping band FWHM of about 160 nm. The mode energy as a function of the incidence angle is reported in the inset of Fig. 3. As the incidence angle increases the cavity mode shows a blue shift due to the increasing photon longitudinal wave vector. The angle dependence of the mode energy is well reproduced by a photon-like dispersion for a cavity with an effective refractive index of 1.451 [19]. This value, slightly higher than the LiF one, is mainly due to the presence of the organic layer whose refractive index, at the wavelength of the cavity, is complex and almost higher than the LiF value. Moreover, this leads to an increased absorbance of the cavity layer thus lowering the Q factor.

The uniformity of the cavity has been checked by measuring the reflectivity in different zones along the sample surface (having a circular shape of diameter 5.5 mm). The mode wavelength dependence on the position on the sample is reported in Fig. 4. The maximum mode wavelength variation is 2.4 nm, which is comparable with the mode linewidth. Moreover, the mode wavelength does not show random oscillations around and average value, instead shows a systematic red shift when moving on the sample from right to left (inset of Fig. 4) and a blue shift when moving in the opposite direction. This is connected to the non-uniform beams shape which induces a systematic and progressive variation of the layer thickness along

the microcavity area and can be removed by using a rotating sample holder to improve the thickness uniformity during the evaporation.

In conclusion we described a novel approach to realize DBR dielectric mirrors fully based on thermal evaporation of LiF and TeO_x. This approach allows us to realize highly reproducible, wide stopping band and high reflectivity mirrors. The wide stopping band of our mirrors makes them particularly interesting to application to organic microcavities, since it allows to obtain single peak luminescence despite the commonly broad luminescence spectrum of organic compounds. Moreover, the thermal evaporation technique is particularly suitable for organic materials deposition due to its cheapness, high controllability, and full compatibility with the active material deposition, which allows a single step fabrication of organic microcavities. Our approach has been tested by realizing high-quality organic microcavities with mode linewidth as small as 1.9 nm, Q-value up to 300 and excellent uniformity over many millimeter square. These results are relevant for application of LiF–TeO_x DBR in organic LEDs, flat panel display and laser resonators.

This work was partially supported by MURST 40%.

References

[1] G. Gu, G. Parthasarathy, P.E. Burrows, P. Tian, I.G. Hill, A. Kahn, S.R. Forrest, J. Appl. Phys. 86 (1999) 4067.
[2] P.E. Burrows, V. Khalfin, G. Gu, S.R. Forrest, Appl. Phys. Lett. 73 (1998) 435.
[3] D.G. Lidzey, M.A. Pate, D.M. Whittaker, D.D.C. Bradley, M.S. Weaver, T.A. Fisher, M.S. Skolnick, Chem. Phys. Lett. 263 (1996) 655.
[4] R.H. Jordan, L.J. Rothberg, A. Dodabalapur, R.E. Slusher, Appl. Phys. Lett. 69 (1996) 1997.
[5] A. Dodabalapur, L.J. Rothberg, R.H. Jordan, T.M. Miller, R.E. Slusher, J.M. Phillips, J. Appl. Phys. 80 (1996) 6954.
[6] J. Gruener, F. Cacialli, I.D.W. Samuel, R.H. Friend, Synth. Methods 76 (1996) 137.
[7] H.F. Wittmann, L. Gruener, R.H. Friend, G.W.C. Spencer, S.C. Moratti, A.B. Holmes, Adv. Math. 7 (1995) 541.
[8] A. Dodabalapur, L.J. Rothberg, T.M. Miller, Kwock, Appl. Phys. Lett. 64 (1994) 2486.
[9] T. Tsutsui, N. Takada, S. Saito, E. Ogino, Appl. Phys. Lett. 65 (1994) 1868.
[10] M.A. Diaz-Garcia, F. Hide, B.J. Schwartz, M.D. McGehee, M.R. Andersson, A.J. Heeger, Appl. Phys. Lett. 70 (1997) 3191.
[11] N. Tessler, G.J. Denton, R.H. Friend, Nature 382 (1996) 695.
[12] D.G. Lidzey, D.D.C. Bradley, T. Virgili, A. Armitage, M.S. Skolnick, S. Walker, Phys. Rev. Lett. 82 (1999) 3316.
[13] T. Virgili, D.G. Lidzey, D.D.C. Bradley, G. Cerullo, S. Stagira, S. De Silvestri, Appl. Phys. Lett. 74 (1999) 2767.
[14] D.G. Lidzey, D.D.C. Bradley, M.S. Skolnick, T. Virgili, S. Walker, D.M. Whittaker, Nature 395 (1998) 53.
[15] A. Arena, S. Patanè, G. Saitta, S. Savasta, R. Girlanda, R. Rinaldi, Appl. Phys. Lett. 72 (1998) 2571.
[16] T. Granlund, M. Theander, M. Berggren, M. Andersson, A. Ruzeckas, V. Sundstrom, G. Bjork, M. Granstrom, O. Inganas, Synth. Methods 102 (1999) 1038.
[17] A. Convertino, A. Valentini, R. Cingolani, Appl. Phys. Lett. 75 (1999) 322.
[18] M. Allegrini, A. Arena, M. Labardi, G. Martino, R. Girlanda, C. Pace, S. Patanè, G. Saitta, S. Savasta, Appl. Surf. Sci. 142 (1999) 603.
[19] M.S. Skolnick, T.A. Fisher, D.M. Whittaker, Semicond. Sci. Technol. 13 (1998) 645.